A geometric morphometric analysis of hominin upper first molar shape

A. Gómez-Robles [a,*], M. Martinón-Torres [a], J.M. Bermúdez de Castro [a], A. Margvelashvili [a,b], M. Bastir [c,d], J.L. Arsuaga [e], A. Pérez-Pérez [f], F. Estebaranz [f], L.M. Martínez [f]

[a] *Centro Nacional de Investigación sobre Evolución Humana (CENIEH), Avda. de la Paz, 28, 09006 Burgos, Spain*
[b] *Georgian National Museum, Purtseladze, 3, 0105 Tbilisi, Georgia*
[c] *Department of Palaeobiology, Museo Nacional de Ciencias Naturales, CSIC. C/José Gutiérrez Abascal 2, 28006 Madrid, Spain*
[d] *Hull York Medical School, The University of York, Heslington, York YO10 5DD, United Kingdom*
[e] *Centro de Evolución y Comportamiento Humanos. C/Sinesio Delgado, 4, pabellón 14, 28029 Madrid, Spain*
[f] *Department on Animal Biology, Section of Anthropology, University of Barcelona, Av. Diagonal 645, 08028 Barcelona, Spain*

Abstract

Recent studies have revealed interesting differences in upper first molar morphology across the hominin fossil record, particularly significant between *H. sapiens* and *H. neanderthalensis*. Usually these analyses have been performed by means of classic morphometric methods, including the measurement of relative cusp areas or the angles defined between cusps. Although these studies have provided valuable information for the morphological characterization of some hominin species, we believe that the analysis of this particular tooth could be more conclusive for taxonomic assignment. In this study, we have applied geometric morphometric methods to explore the morphological variability of the upper first molar (M^1) across the human fossil record. Our emphasis focuses on the study of the phenetic relationships among the European middle Pleistocene populations (designated as *H. heidelbergensis*) with *H. neanderthalensis* and *H. sapiens*, but the inclusion of *Australopithecus* and early *Homo* specimens has helped us to assess the polarity of the observed traits. *H. neanderthalensis* presents a unique morphology characterized by a relatively distal displacement of the lingual cusps and protrusion in the external outline of a large and bulging hypocone. This morphology can be found in a less pronounced degree in the European early and middle Pleistocene populations, and reaches its maximum expression with the *H. neanderthalensis* lineage. In contrast, modern humans retain the primitive morphology with a square occlusal polygon associated with a round external outline.

Keywords: Neandertals; Dental anthropology; Geometric morphometrics; Maxillary molars

Introduction

Teeth are a valuable and durable source of information for anthropological research based, on the one hand, on their abundance and excellent preservation in the fossil record (e.g., Butler, 1963; Larsen and Kelley, 1991). The scope of dental anthropology ranges from ecological studies (e.g., Molnar, 1971; Hillson, 1986; Lalueza and Pérez-Pérez, 1993; Pérez-Pérez et al., 2003; Lozano et al., 2004) to the characterization of species (e.g., Weidenreich, 1937; Le Gros Clark, 1950; Tobias, 1991) and the reconstruction of their relationships (e.g., Irish, 1997, 1998; Bailey, 2000, 2002; Irish and Guatelli-Steinberg, 2003). Moreover, teeth do not suffer remodellation in response to environmental stresses as other skeletal parts do (Dahlberg, 1971; Larsen and Kelley, 1991; Thomason, 1997), so once they are formed, their morphology is only affected by attrition or decay. Therefore, teeth are excellent and stable markers for affinity studies within and among populations (Turner, 1969) and, thus, for the study of human ancestors (Irish, 1993). Among other things, dental anthropology investigates the taxonomic utility of teeth, searching for morphometric traits that may be useful in characterizing hominin groups.

The origin of *H. sapiens*, our relationship with *H. neanderthalensis*, and the identification of our last common ancestor is still an open debate (e.g., Bermúdez de Castro et al., 1997; Foley and Lahr, 1997; Lahr and Foley, 1998; Rightmire, 1998; Stringer and Hublin, 1999; Stringer, 2002). Thus, it is necessary to search for morphological traits that establish the similarities and differences among the groups under discussion. We contribute to this debate by comparing modern humans and Neandertals with the crucial inclusion of the large dental sample from Atapuerca-Sima de los Huesos site that are representative of *H. heidelbergensis* and considered direct ancestors of *H. neanderthalensis* (Arsuaga et al., 1997), and from the Atapuerca-TD6 sample, the only dental remains recovered, so far, from the European early Pleistocene (Bermúdez de Castro et al., 1997). In addition, we also include a large sample of teeth assigned to several species of the genera *Australopithecus* and *Homo* in order to explore the polarity of the observed morphologies.

In dental anthropological studies, upper first molars (M^1) are potentially useful for taxonomic assignment of isolated human remains (e.g., Wood and Engleman, 1988; Tattersall and Schwartz, 1999; Bailey, 2004) and are even distinct among different modern human populations (Morris, 1986). Moreover, M^1 morphology has been shown to be distinctive in *H. neanderthalensis* (Bailey, 2004). These conclusions usually come from personal observation and classic metric studies using linear measurements of the crown (Morris, 1986; Wood and Engleman, 1988), cusps angles (Morris, 1986; Bailey, 2004), relative cusp areas (Wood and Engleman, 1988; Bailey, 2004), and occlusal polygon areas (defined by lines connecting cusp apices; Morris, 1986; Bailey, 2004). In addition, M^1 displays the most stable morphology within the molar series (Scott and Turner, 1997), which undoubtedly makes it easier to identify homologous landmarks despite variation among species.

The Arizona State University Dental Anthropology System (ASUDAS; Turner et al., 1991) is one of the standards developed to assess modern human dental variability and it has been also applied to other fossil hominin species with moderate success (e.g., Irish, 1997, 1998; Bailey, 2000, 2002; Irish and Guatelli-Steinberg, 2003). However, this system fails to cover the complete range of dental variation in the hominin fossil record (Bailey, 2002, 2004; Hlusko, 2004; Martinón-Torres, 2006), particularly in the case of the upper first molar. Furthermore, classic morphometric studies have also revealed certain limitations for characterizing the dental variability of some populations (e.g., Goose, 1963; Hillson et al., 2005; Stojanowski, 2006), motivating the search for alternative methods with different degrees of success (Biggerstaff, 1969; Morris, 1986; Mayhall, 2000; Bailey, 2004; Hillson et al., 2005; Stojanowski, 2006).

In relation to this matter, geometric morphometric techniques have been proven to be effective tools for measuring shape variation, allowing powerful statistical comparisons (Rohlf and Marcus, 1993). Therefore, their application to dental studies might advance our knowledge of dental morphological variability and its evolutionary significance. The possibility of finding apomorphic traits for characterizing paleospecies (Wolpoff, 1971; Bytnar et al., 1994; Bailey, 2000, 2002, 2004; Bailey and Lynch, 2005) makes it worthwhile to explore alternative methodologies. In the dental field, geometric morphometrics overcomes some methodological difficulties related to absolute tooth orientation within the jaw and helps us to understand outline shape variation with respect to biologically meaningful structures, such as the spatial configuration of cusps, and their relationship to overall size (Martinón-Torres et al., 2006).

The aim of our study is to evaluate the phenetic relationships among European middle Pleistocene populations, *H. neanderthalensis* and *H. sapiens*, exploring the differences in M^1 morphology and among these species by means of geometric morphometrics. Previous studies lacked samples large enough to ascertain primitive *versus* derived nature of the M^1 shape variation (Bailey, 2002, 2004). The inclusion of a sample of early *Homo* and *Australopithecus* in the comparison will help to determinate the polarity of the morphological variants and whether these differences have any utility in the taxonomic assignment of specimens.

Materials and methods

Materials and photographic methods

We performed a geometric morphometric analysis on a sample of 105 M^1s from several hominin species with special emphasis on *H. heidelbergensis*, *H. neanderthalensis* and *H. sapiens*. The sample included (Table 1): *Australopithecus anamensis* ($n = 2$), *A. afarensis* ($n = 6$), *A. africanus* ($n = 10$), *Homo habilis sensu lato* ($n = 10$), *H. ergaster* ($n = 4$), *H. erectus* ($n = 5$), *H. georgicus* ($n = 2$), *H. antecessor* ($n = 3$), *H. heidelbergensis* ($n = 16$), *H. neanderthalensis* ($n = 14$), and *H. sapiens* ($n = 32$).

The inclusion of *Australopithecus* and other Pliocene and Pleistocene *Homo* specimens in the comparison helped us to assess the phylogenetic significance of the observed differences. *Australopithecus* species were analyzed separately. For comparative purposes, specimens usually ascribed to *H. habilis* and *H. rudolfensis*, as well as some African Pliocene specimens without consensus in their taxonomical assignment, were grouped as *H. habilis s.l.* The African specimens attributed by some authors to *H. erectus sensu lato* (Walker and Leakey, 1993) were analyzed as *H. ergaster* (Groves and Mazák, 1975), leaving the denomination *H. erectus* (Dubois, 1894) for the Asian specimens (Andrews, 1984; Stringer, 1984; Wood, 1984). A North African early middle Pleistocene specimen assigned to *H. mauritanicus* by Hublin (2001) was included in *H. ergaster*. We used the denomination *H. georgicus* for the Dmanisi hominins (Gabunia et al., 2002) and *H. antecessor* (Bermúdez de Castro et al., 1997) for the European early Pleistocene specimens from Atapuerca-TD6. Hominins from the European middle Pleistocene were grouped as *H. heidelbergensis*, and the *H. neanderthalensis* taxon comprised classic late Pleistocene European Neandertals. Finally, the *H. sapiens* sample included a medieval collection from the San Nicolás site (Murcia, Spain; González, 1990) and specimens from several European Upper Paleolithic sites.

Table 1
List of the specimens included in this analysis

Australopithecus anamensis ($n=2$)	ER30200; ER31400 (casts)
Australopithecus afarensis ($n=6$)	AL200; AL486; LH3H; LH6; LH17; LH21 (casts)
Australopithecus africanus ($n=10$)	MLD6; TM1511; STS1; STS8; STS21; STS52; STS56; STS57; STW151; STW183 (casts)
Homo habilis s.l. ($n=10$)	SE255; ER808; ER1590; ER1813; OH6; OH13; OH21; OH39, OH41; OH44 (casts)
Homo georgicus ($n=2$)	D2282; D2700 (originals)
Homo ergaster ($n=4$)	SK27; SKX268; WT15000; Rabat (casts)
Homo erectus ($n=5$)	Sangiran 7-3; 7-9; 7-10; 7-37; 7-40 (casts)
Homo antecessor ($n=3$)	ATD6-18; ATD6-69; ATD6-103 (originals)
Homo heidelbergensis ($n=16$)	Arago 9; 54 (casts) Sima de los Huesos: AT-1100; AT-16; AT-196; AT-20; AT-2071; AT-26; AT-3177; AT-587; AT-767; AT-772; AT-812 (originals) Pontnewydd: 4; 12 (casts) Steinheim (cast)
Homo neandertalensis ($n=14$)	Krapina: MxA; MxB; 100; 134; 136; 166; 171; (casts) Pinilla del Valle: PIN10 (original) Kulna: Kulna 1 (cast) Le Moustier: Le Moustier 1 (cast) Saint Cesaire: SC; SC1 (casts) Sidrón: SDR012 (cast) Tabun: TB1 (C1) (cast)
Homo sapiens ($n=32$)	Mladec: Mladec 1 (cast) Jebel Iroud (cast) Almonda (cast) Trou Magritte (cast) Abri Pataud: Pataud 1 (cast) Dolni Vestonice 13; 14; 15 (originals) Medieval modern human collection from Universidad Autónoma de Madrid (originals)

Environmental stresses may influence the development of the genetic pattern in both antimeres resulting in fluctuating asymmetry (Waddington, 1957). However, asymmetry in dental morphology tends to be minor and does not imply heterozygosity (Trinkaus, 1978; Scott and Turner, 1997). We randomly chose the left antimere for these analyses. In order to maximize sample sizes, when the left tooth was absent or when the landmarks were less clear, the right tooth was mirror-imaged with Adobe Photoshop®. Teeth with severe attritional wear were not included.

We used standardized occlusal surface pictures of the M^1. Images were taken with a Nikon® D1H digital camera fitted with an AF Micro-Nikon 105 mm, f/2.8D. The camera was attached to a Kaiser Copy Stand Kit RS-1® with grid baseboard, column, and adjustable camera arm, ensuring that the lens was parallel to the baseboard and the cementoenamel junction (CEJ). For maximum depth of field, we used an aperture of f/32. The magnification ratio was adjusted to 1:1, and a scale was included and placed parallel to, and at the same distance from the lens as, the occlusal plane.

Some authors have pointed to some problems that may derive from working on 2D projections of 3D objects, such as the possible distortion of the original size and shape of the structures (Frieß, 2003) and the orientation of the photographed elements (Gharaibeh, 2005). Although, ideally, this type of study should be performed directly on 3D structures, there are an important number of dental morphological studies that have been successfully performed on 2D images of the teeth (Bailey, 2004; Bailey and Lynch, 2005; Martinón-Torres et al., 2006; Pérez et al., 2006, among the most recent).

Geometric morphometric methods

Geometric morphometrics capture the spatial aspects of morphological variation of biological structures. Shape variation in morphological structures is captured by configurations of landmarks, which are points of correspondence between different objects that match between and within populations (Bookstein, 1991; O'Higgins, 2000; Zelditch et al., 2004). Landmarks have both coordinates and a biological significance (Bookstein, 1991). Generalized Procrustes superimposition (GPA; Sneath, 1967; Rohlf and Slice, 1990; Dryden and Mardia, 1998) produces a common *consensus* or mean configuration of the studied sample by iteratively minimizing the distances between corresponding landmarks using least-squares methods, after translation, rotation, and scaling of the configurations. The results of the generalized Procrustes superimposition are scatters of corresponding landmarks (Procrustes shape coordinates) around their means. The shape of a Procrustes registered landmark configuration is defined by the entirety of its residual coordinates (Zelditch et al., 2004).

Thin-plate spline (TPS) provides another representation of the shape differences between two objects by a deformation of the first specimen into the second one. The total deformation between two particular specimens or between a specimen and the *consensus* configuration can be partitioned into a uniform and a non-uniform component. The uniform component affects the whole configuration of landmarks in the same manner such as is the case with shearing. The non-uniform component requires bending energy and contributes to the deformation of specific regions of the structure (Bookstein, 1991). The properties of this bending energy can be used to derive a set of powerful shape descriptors, the partial warps plus the uniform component (Bookstein, 1989, 1991, 1996a; Rohlf, 1996).

Finally, relative warps analysis (Bookstein, 1991) corresponds to a principal components analysis of the partial warp scores and illustrates the main patterns of morphological variation. Given its similarity to principal components analysis, relative warps are a useful tool for exploring variation, and they serve to reduce the total variation to a smaller number of independent dimensions (Frieß, 2003). Typically, the first few components (or relative warps) summarize most of the variation of a sample (Frieß, 2003). The relative warps analysis was performed using TpsRelw software (Rohlf, 1998a).

More detailed information about this method and its applications can be found in other texts (e.g., Bookstein, 1989, 1991, 1996a; Rohlf and Slice, 1990; Rohlf, 1996; Bookstein et al., 1999, 2003: Bastir et al., 2004, 2005).

Canonical variates analysis

To better understand the variability of our sample we performed a canonical variates analysis (CVA), appropriate to obtain an optical discrimination among groups relative to variation within groups, in as much as the individuals can be organized in mutually exclusive groups (Zelditch et al., 2004). This type of analysis is highly recommended in studies where the variation among individuals is high, since it maximizes intergroup variability relative to intragroup variability (Albrecht, 1980).

In order to have a significant representation of the intragroup variability, the CVA was only performed for those groups with a sample size greater than ten (i.e., *A. africanus*, *H. habilis s.l.*, *H. heidelbergensis*, *H. neanderthalensis*, and *H. sapiens*). The CVA was performed employing a generalization of Fisher's linear discriminant function, to determinate a linear combination from the original variables which maximizes intergroup variability (Mardia et al., 1979). Since the CVA describes differences among groups, its results and interpretations may differ from those obtained with the PCA. In addition, CVA implies a rescaling and reorientation of the axis maximizing intergroup variance relative to intragroup variance (Zelditch et al., 2004). We employed the TpsRegr software (Rohlf, 1998b) for multivariate regression of shape data on CV scores to visualize the shape associated to a given canonical axis.

From the CVA, an assignment test was performed. With this test, each individual is assigned to one of the pre-established groups, calculating the probability of the Mahalanobis distance between each individual and its group mean being lower than the expected distance under the null hypothesis of random variation (Zelditch et al., 2004). This type of test is employed to evaluate the utility of the axis derived from the CVA, to discriminate and determine the affinity of the groups established *a priori* (Nolte and Sheets, 2005).

Landmarks and semilandmarks

As we mentioned above, landmarks are points of biological and geometric correspondence among specimens (Zelditch et al., 2004). In 2D space they have two clear coordinates. Landmarks should be chosen according to their utility in assessing morphological variability and their ease of identification for location and relocation without error (Zelditch et al., 2004). In this study, four landmarks were chosen on the occlusal surface of M^1 (Biggerstaff, 1969), corresponding to the tips of the four main cusps (Fig. 1): landmark 1: tip of the mesiolingual cusp or protocone; landmark 2: tip of the mesiobuccal cusp or paracone; landmark 3: tip of the distobuccal cusp or metacone; and landmark 4: tip of the distolingual cusp or hypocone.

The digitization of the landmarks was performed by A. G.-R. using the TpsDig software (Rohlf, 1998c). When using a cast, the tips of the main cusps were marked with soft pencil prior to photographing. When using an original or when permission to mark was denied, the tips of the main cusps were visually located in the images while simultaneously examining the fossil. When the teeth showed little wear, the cusp tip was marked in the center of the wear facet. When mesial and/or distal borders of the teeth were affected by light interproximal wear, original borders were estimated by reference to overall crown shape and

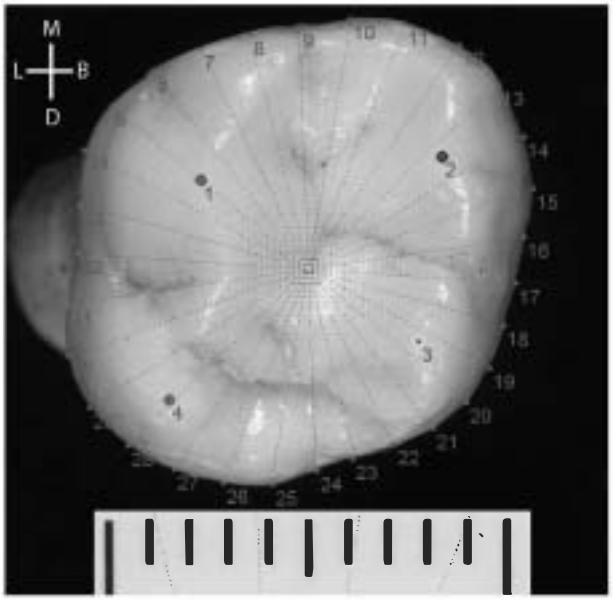

Fig. 1. TpsDig digitized image of a left upper first molar of *H. heidelbergensis* (SH) showing the four landmarks: (1) protocone tip; (2) paracone tip; (3) metacone tip; (4) hypocone tip; and the 30 semilandmarks (5 to 34) located at the intersection of the external outline and the fan lines. M = mesial, D = distal, B = buccal, L = lingual.

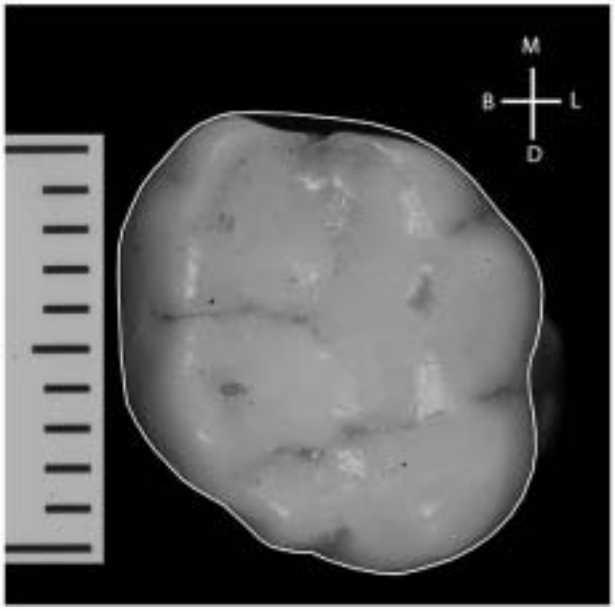

Fig. 2. Sima de los Huesos right upper first molar corrected for interproximal wear. M = mesial, D = distal, B = buccal, L = lingual.

the buccolingual extent of the wear facets (Fig. 2), following Wood and Engleman (1988) and Bailey (2004).

The use of sliding semilandmarks was introduced by Bookstein with the aim to use "landmarks for description of structures that lack *true* landmarks" (Bookstein, 1997; Bookstein et al., 1999). Recently, they have been increasingly used in morphological studies (Mitteroecker et al., 2004, 2005; Sheets et al., 2004; Gunz et al., 2005; Bastir et al., 2006; Martinón-Torres et al., 2006; Pérez et al., 2006). Semilandmarks are particularly useful in dental studies, where relevant information such as asymmetry or contour shape (Wood et al., 1983; Wood and Uytterschaut, 1987; Bailey and Lynch, 2005; Martinón-Torres et al., 2006) cannot be defined by landmarks.

For the assessment of the external outline of the M^1s, we employed a set of 30 semilandmarks. Semilandmarks are characterized by one well-defined coordinate on the curve and one arbitrary one. Therefore, they have been defined as "mathematically deficient" to some degree (Bookstein, 1991, 1997), but still useful to explore shape difference in structures which are not biologically significant (Adams et al., 2004). "Sliding techniques" are employed to minimize the effects of the arbitrary location of the semilandmarks along the curve (Bookstein, 1996b, 1997; Bookstein et al., 2002; Gunz et al., 2005). This technique extends the standard Procrustes superimposition method, sliding the points along the external curve until they correspond optimally to their equivalents in the *consensus* configuration (Bookstein, 1997). The semilandmarks can be slid along tangents defined by neighboring semilandmarks, either to minimize bending energy (Bookstein, 1997; Bookstein et al., 2002, 2003; Mitteroecker et al., 2004; Bastir et al., 2006) or, as in this study, Procrustes distance (Rohlf, 1998a). Sliding techniques help to minimize the arbitrary part of variation (Rohlf, 1998a). After the Procrustes fit, the semilandmarks are in comparable positions describing a homologous curve within the Procrustes superimposed sample (Bookstein, 1996b, 1997), and from that moment they can be statistically analyzed as true landmarks (Adams et al., 2004; Martinón-Torres et al., 2006). The sliding technique provides nonarbitrary criteria (Zelditch et al., 2004; Gunz et al., 2005) and allows curves or outlines to be analyzed within the Procrustes scheme of shape analysis (Rohlf and Slice, 1990; Slice, 2001; Rohlf, 2003). However, it is important to keep in mind that no standardized protocol has yet been developed for the use of sliding semilandmarks, and further research needs to be done to address this issue (Martinón-Torres et al., 2006; Pérez et al., 2006).

Based on the position of the four landmarks, the MakeFan6 software (Sheets, 2001) localized a centroid, from which 30 equiangular fan lines were drawn. Then, the semilandmarks were located at the intersection of the external outline of the M^1 and the fan lines.

Allometry and internal/external shape correlation

The centroid size is defined as the squared root of the sum of squared distances of a set of landmarks from their centroid and is a measure of scale (Zelditch et al., 2004). The centroid of a configuration is its "gravity center", and its coordinates are the mean of all the landmarks' coordinates. Thus, the centroid size is a measurement of the dispersion of the landmarks around the centroid (Zelditch et al., 2004).

To test for allometry, we used the TpsRegr software (Rohlf, 1998b) to perform a multivariate regression analysis of partial warps and uniform components scores on centroid size.

In order to better understand the ontogeny of shape variation, we tested the correlation between the internal and external configurations (determined by the landmarks and the semilandmarks conformation, respectively), that is, the influence that the cusps' size and location may have on the outline shape. For that purpose we used the TpsPLS software (Rohlf, 1998d), employed to explore the relationships between the variation of two shapes or between one shape and a set of variables recorded from the same specimen, being especially interested in its ability to evaluate the covariation between two different configurations of points (Rohlf, 1998d).

Statistical error, repeatability, and the use of worn teeth

To assess the possible measurement error tied to the digitizing process, the complete data recording procedure of a random subsample of five specimens was repeated during two sets of five days (see Martinón-Torres et al., 2006), separated by four months, in order to avoid an unrealistically low error due to a familiarization with the teeth during consecutive five days. TpsUtil software (Rohlf, 1998e) was used to randomize the order of the data by the computer, and the first five specimens of the random data set were selected. This random test-sample comprised four fossils (AT-2071, AT-196, STS52, PIN10) and one modern human (MH-548). The complete digitization process was repeated every day for every

individual, obtaining ten Procrustes distances matrices. The accuracy of the digitization was analyzed by means of a Mantel test (Mantel, 1967), which measured the correlation among the Procrustes distances matrixes obtained during each day of measurement.

The correlation among Procrustes matrices for each day of measurements has a mean value of 0.991, with values ranging between 0.975 and 0.999. The correlation mean value for the first and second sets of five days was 0.996 and 0.993, respectively, with a slightly lower value for the interset comparisons (0.989).

Ideally, this type of study should be performed on unworn teeth but this would drastically reduce the sample size, nearly precluding any significant analysis. Although teeth with severe attrition were not included, some of the analyzed teeth exhibit some wear. In order to test the error introduced by the analysis of teeth with moderate wear degree, we performed a full factorial MANCOVA, employing the factor *species*, the factor *dental wear*, and the interaction between both variables as independent factors. We used as dependent variables the partial warps and the uniform component scores.

In these samples, three factor levels were used to categorize occlusal wear: (1) total absence of wear, (2) light wear, and (3) the maximum wear allowed. Six levels categorized the species factor: *A. afarensis*, *A. africanus*, *H. habilis s.l.*, *H. heidelbergensis*, *H. neanderthalensis*, and *H. sapiens*. With this model, we assessed whether molar shape depends on the species, on the degree of wear of the analyzed sample, or on the degree of wear within each species. We tested the interaction between the *wear degree* and the *species* factors, to check how the inclusion of worn teeth may influence each subsample and the total sample. With this analysis we intend to avoid the potential influence of differential wear among species. For this reason, in these analyses we included only groups with a sample size large enough to perform statistical analysis when worn teeth are excluded.

In general, the degree of wear does not significantly influence M^1 morphology, either within or among species. Total shape does not depend on the degree of wear ($F = 1.2333$, $p = 0.4044$) nor on the degree of wear within a species ($F = 1.1988$, $p = 0.1352$). The model shows, however, that the total shape depends signficantly on the species factor ($F = 2.4727$, $p = 0.0010$).

In addition to the previous test, we have performed a relative warps analysis carried out exclusively with the unworn specimens and the results are provided below.

Results

Relative warps analysis

The relative warps analysis reveals that the first two principal components account for 40.2% of the total variation of the sample (PC1: 21.1%; PC2: 19.0%). Table 2 displays the singular values and the percentage of the explained variance by each of the ten first principal components.

Figure 3 illustrates the morphological variation of the M^1 along the first two principal components. Specimens with negativePC1 values are characterized by an approximately squared occlusal polygon, with nearly right angles, and a regular external contour. The distance between the protocone and the hypocone is equal to or even lower than the distance between the paracone and the metacone. Specimens with positive PC1 values are characterized by a relatively distal displacement of the lingual cusps, especially the hypocone, so that the angles formed at the hypocone and the paracone are more acute while those at the protocone and the metacone are more obtuse. This results in a skewed contour in which the hypocone causes a bulging of the external outline. Relative enlargement of the protocone-hypocone distance with regard to the paracone-metacone distance can be observed in the TPS-grids. The relative lengthening of this distance can be measured by calculating the ratio between the paracone-metacone distance and the protocone-hypocone distance, showing significant variation among species ($p > 0.0000$). Pliocene and early Pleistocene specimens display higher mean values for this proportion, thus reflecting a shorter protocone-hypocone distance (*A. afarensis:* 0.83; *A. africanus:* 0.80; *H. habilis s.l.:* 0.78). The lowest mean values are displayed by the European groups (*H. heidelbergensis:* 0.71; *H. neanderthalensis:* 0.69) and *H. sapiens* presents an intermediate mean value (0.73).

Positive loading on PC2 is associated with a slight displacement of the occlusal polygon towards the distal face, whereas

Table 2
Relative warps (RW) analysis with the total sample and after removing worn specimens. The table displays the first ten principal components, the singular values, and the percentage of explained variance for both analyses

No.	With worn molars			Without worn molars		
	Singular value	% Explained variance	% Cumulative variance	Singular value	% Explained variance	% Cumulative variance
1	0.24	21.14	21.14	0.20	22.34	22.34
2	0.23	19.05	40.19	0.19	21.06	43.40
3	0.22	17.63	57.82	0.17	17.83	61.23
4	0.15	8.70	66.52	0.12	8.75	69.98
5	0.14	7.32	73.84	0.10	6.30	76.28
6	0.12	5.80	79.64	0.09	4.74	81.02
7	0.10	3.95	83.59	0.08	4.14	85.15
8	0.09	2.81	86.39	0.07	2.91	88.06
9	0.08	2.38	88.77	0.06	2.03	90.09
10	0.07	1.83	90.60	0.05	1.77	91.85

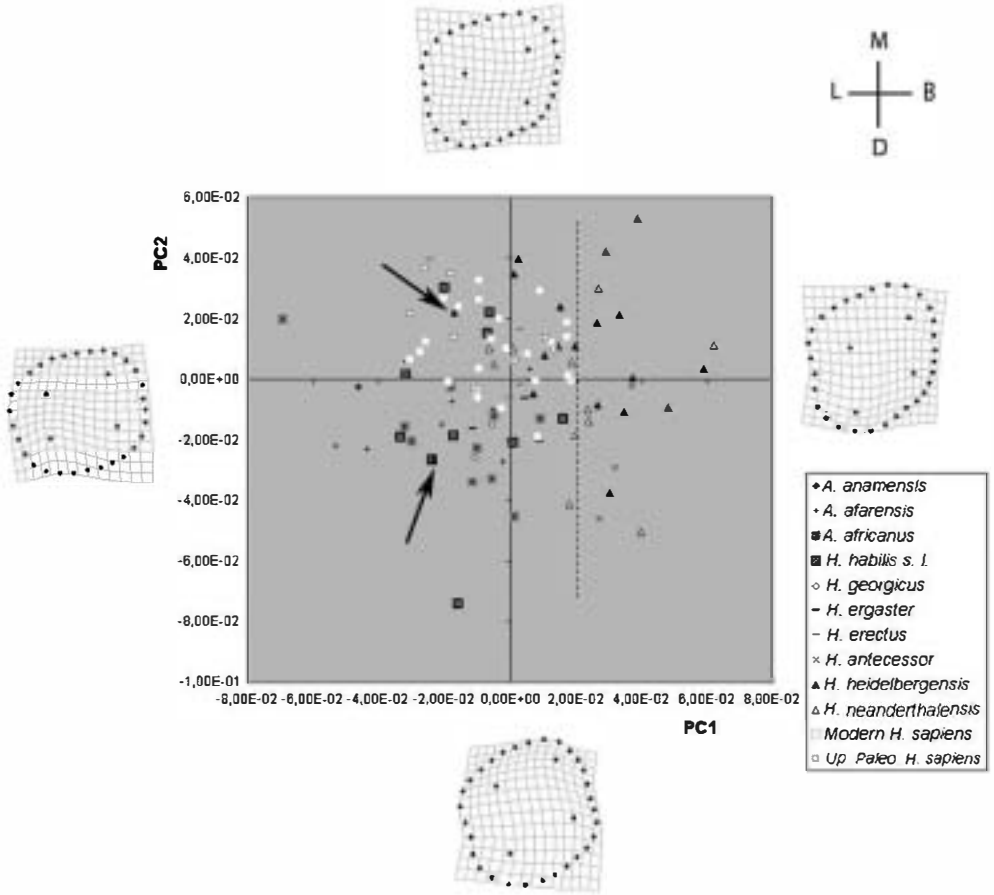

Fig. 3. Projection of individual M^1s crowns on PC1 and PC2. In the extremes of the axis, TPS-grids illustrate the morphological variation trends of the specimens along each principal component. These grids show how a TPS transformation of the mean shape into a theoretical specimen would look if its PC-score were at an extreme point of the one PC axis and zero at all other axes. The dotted line outlines the concentration of *H. heidelbergensis* and *H. neanderthalensis* specimens, which might be illustrating a derived morphology in these species. The arrows are pointing to the Arago molars, which show a more primitive morphology than most of the *H. heidelbergensis* specimens (see text for explanation). M = mesial, D = distal, B = buccal, L = lingual.

negative loading is associated with a buccal displacement and enlargement of the occlusal polygon, especially due to a more external location of the protocone.

H. neanderthalensis and *H. heidelbergensis* plot mainly in the positive extreme of PC1 axis (Fig. 3). Twelve of the fourteen *H. neanderthalensis* specimens display positive values on PC1, and both specimens with negative PC1 values are very close to zero. More than two-thirds of the *H. heidelbergensis* specimens (14 out of 16) exhibit positive values for PC1. Interestingly, the two *H. heidelbergensis* specimens with negative values on PC1 are from Arago, whereas all the Atapuerca-SH specimens, as well as those from Pontnewydd and Steinheim, cluster together on the positive side of PC1. *H. sapiens* plot throughout the four quadrants but are absent from the positive extreme of the PC1 axis and the negative extreme of PC2. The *H. sapiens* specimens from several European Upper Paleolithic sites occupy the complete range of variation seen in *H. sapiens* for the PC1, and they have almost exclusively positive values for PC2. Clustered with *H. heidelbergensis* and *H. neanderthalensis* M^1s, we find the three specimens assigned to *H. antecessor*. *H. habilis s.l.* specimens are scattered mainly on the negative side of the PC1, with eight out of ten molars showing negative values for this PC. *A. afarensis* and *A. africanus* have mostly negative values for both principal components, and *H. georgicus* and *A. anamensis* samples plot with negative loadings on both axes. Four out of the five *H. erectus* specimens plot near the zero value of PC1 and PC2 (matching the consensus shape of the sample), whereas *H. ergaster* occupy a wide range for PC1.

The repetition of the relative warps analysis including exclusively the unworn M^1s showed the same distribution pattern (Table 2; Fig. 4). All the *H. neanderthalensis* molars take positive values for the PC1, with virtually no overlap with *H. sapiens* molars. The complete *H. heidelbergensis* sample is plotted on the positive side of PC1, with the exception of one Arago and one Atapuerca-SH individual. The *H. sapiens* sample displays almost the same distribution pattern in both analyses, with most specimens taking negative values for PC1, as is the case with the majority of the primitive specimens. With this analysis, the two unworn *H. antecessor* specimens cluster again with *H. heidelbergensis* and *H. neanderthalensis* in an exclusive area.

The observation of the TPS-grids and an experimental rotation of two specimens of extreme-morphology (LH3H and Kulna1) showed that PC2 retains a certain degree of relation with the orientation of the molars in the photographs, related to the mesiodistal turn of the molar. Although this distortion

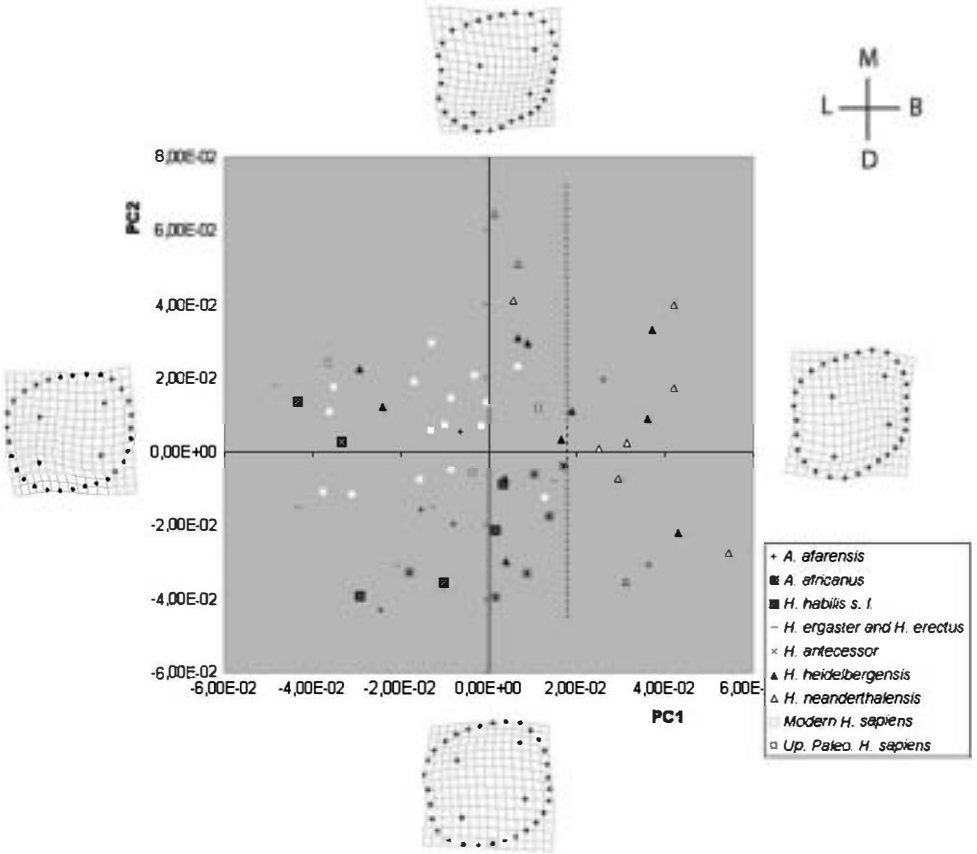

Fig. 4. Projection of individual M^1s crowns on PC1 and PC2 after removing the worn molars. Specimens display essentially the same distribution as in the PCA obtained after analysing the whole sample (unworn and moderately worn specimens; see Fig. 3).

is obviously not desirable, PC2 is the axis on which we do not find a clear distribution pattern for the specimens relative to species and, therefore, this distortion should have no influence on these results.

Canonical variates analysis

The CVA extracted four variables that explain the total variation of the analyzed subsample (Table 3). Figure 5 represents the first two canonical variates, which explain 86.2% of the variation among groups relative to the variation within groups. Although the variability explained by the canonical variates (CV) does not necessarily fit the variability explained by the principal component analysis, in this case we can see that there is good correspondence between the TPS-grid conformations at the extremes of the CV1 and the conformations at the extremes of the PC1.

The positive loading on the CV1, along the x-axis, shows the distal displacement of the lingual cusps and, therefore, the protrusion of the hypocone into the external contour and the internal displacement and reduction of the metacone described by Bailey (2004); whereas negative values correspond to a squared occlusal polygon with a regular and smooth contour. The CV2, along the y-axis, shows that positive loadings are related to a centered occlusal polygon and a slight distal displacement of the lingual cusps without the relative lengthening of the protocone-hypocone distance, whereas the negative extreme is characterized by a general expansion of the distal surface without reduction of the metacone and a buccal displacement of an expanded occlusal polygon.

Figure 5 shows certain overlap between the distribution of *A. africanus* and early *Homo*, both of which display exclusively negative values for CV1. *H. sapiens* occupies an intermediate position, with a similar proportion of individuals having positive and negative values on CV1, but with a large majority of positive values on CV2 (24 out of 32). Finally, *H. heidelbergensis* and *H. neanderthalensis* display positive values for CV1. There is a considerable overlap between both species, although *H. neanderthalensis* tends to display higher positive values on CV1 than does *H. heidelbergensis*.

Table 4 displays the results of the assignment test. As we can see, for *A. africanus* the percentage of individuals that are correctly assigned is high. However, the percentage

Table 3
Canonical variates analysis (CVA). This table displays the four functions obtained, their eigenvalues, and the percentage of explained variance

Function	Eigenvalue	% Explained variance	% Cumulative variance
1	2.237	66.6	66.6
2	0.658	19.6	86.2
3	0.443	13.2	99.3
4	0.022	0.7	100.0

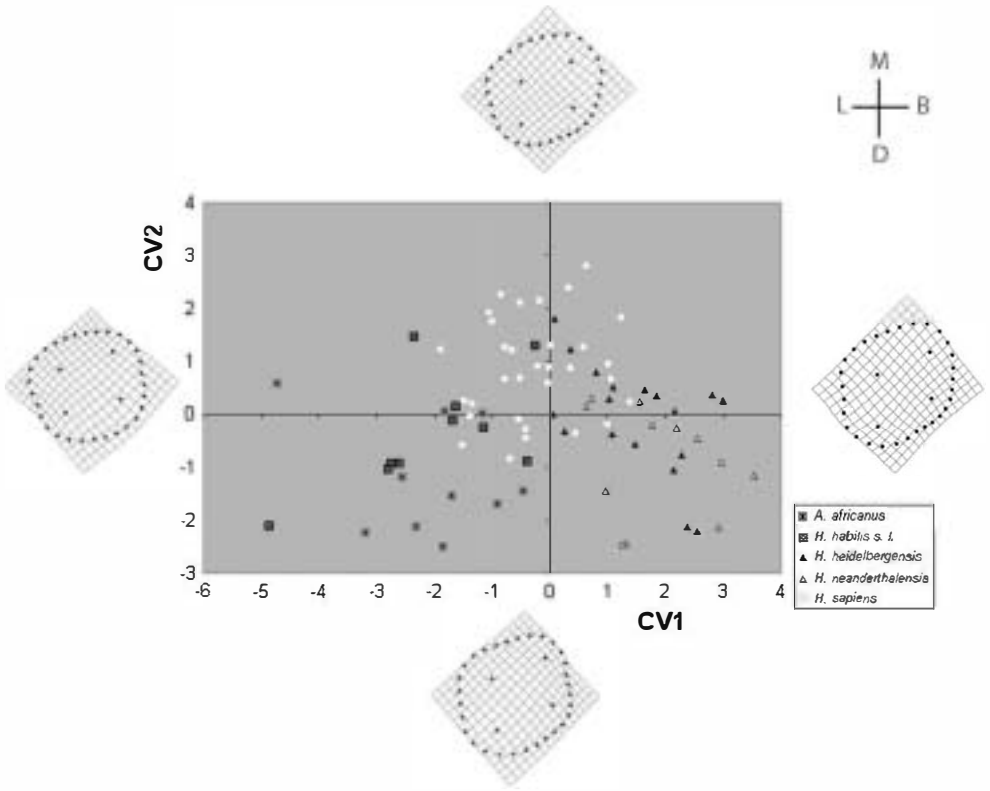

Fig. 5. Canonical variates analysis. The plot displays the projection of the individuals depending on the two first canonical variates, and the TPS-grids show the different conformations corresponding to the extreme of each canonical variates (see text for further explanation).

correctly assigned to *H. habilis s.l.*, *H. heidelbergensis*, *H. neanderthalensis*, and *H. sapiens* is moderate. In *H. habilis s.l.* this may reflect the fact that this group is an amalgamation of specimens based on their geographic and chronological proximity rather than their taxonomic distribution. Interestingly, the majority of the incorrectly assigned *H. heidelbergensis* specimens are assigned to the *H. neanderthalensis* group and vice-versa. This association emphasizes the morphological similarity between these two groups, as does the principal component analysis. With regard to *H. sapiens*, ten specimens were misclassified, but just one of these was assigned to *H. neanderthalensis*, highlighting the morphological differences between these groups.

Allometry and internal/external shape correlation

In general, *H. sapiens*, *H. neanderthalensis*, and *H. heidelbergensis* species have smaller centroid sizes (3.17, 3.49, and 3.39, respectively) than do the African Plio-Pleistocene species (3.82 for *A. afarensis*, 3.89 for *A. africanus*, and 3.53 for *H. habilis*) ($p > 0.000$).

Although the regression analysis shows a very low correlation between the first and second relative warps and centroid size ($r = 0.097$ with the first relative warp and $r = 0.310$ with the second), the regression analysis performed as a multivariate test predicting shape variation as a function of the centroid size (Rohlf, 1998b) revealed a slight but significant allometry ($p > 0.0000$) that accounts for 3.02% of overall variation. Smaller molars show a slight tendency toward displaying a centered, compressed, and rhomboidal occlusal polygon, whereas larger molars tend to show an expanded occlusal polygon with a more squared shape and a relative displacement towards the mesiobuccal vertex (Fig. 6).

The analysis of the covariation between the internal conformation (defined by the four cusp tip landmarks) and the external conformation (defined by the 30 semilandmarks) yields a correlation coefficient of 0.63, showing that both conformations are not independent. As mentioned before, when the four landmarks form a relatively squared occlusal polygon, the external outline tends to be regular and smooth without the protrusion of any cusp. The distal displacement of the hypocone that seems to characterize the *H. heidelbergensis* and *H. neanderthalensis* individuals (Fig. 3) and the internal placement of the metacone described by Bailey (2004) are responsible of the distolingual protrusion in the external outline.

Table 4
Correct assignment percentage obtained in the assignment test based on the canonical variates analysis (CVA)

	% Correct assignment	*N*
A. africanus	90.0	$n = 10$
H. habilis s.l.	80.0	$n = 10$
H. heidelbergensis	50.0	$n = 16$
H. neanderthalensis	78.6	$n = 14$
H. sapiens	68.8	$n = 32$

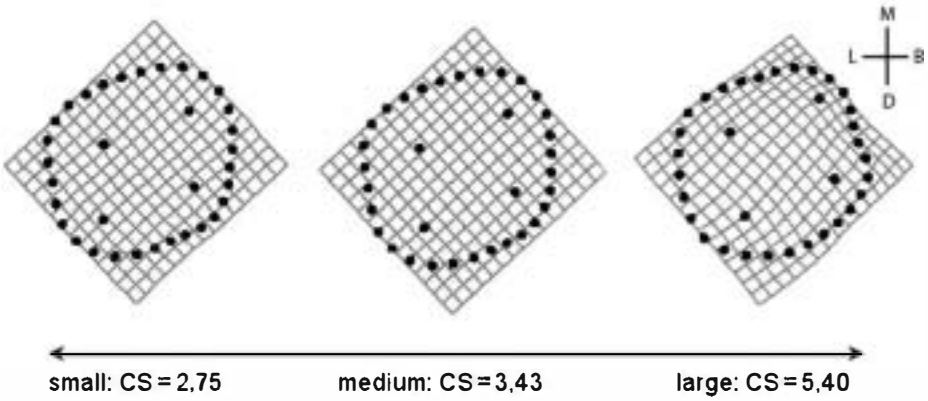

Fig. 6. Morphological variants related to variation in centroid size. The TPS-grids show the theoretical transformation of the mean shape (central image) into a smaller (left) and a larger specimen (right).

Discussion

M^1 morphology: phylogenetic and taxonomic utility

Bailey (2004) pointed out the existence of a distinct morphology in the M^1s of *H. neanderthalensis* based on the comparison of the angles formed by adjacent cusps and relative cusp areas. With an enlarged hominin sample we can affirm that this morphology is not exclusive to *H. neanderthalensis* but is also present in the European early and middle Pleistocene populations. We can also show that the primitive pattern combines an approximately squared occlusal polygon with a regular contour without any particular cusp protrusion. This is the pattern developed by *Australopithecus* and early *Homo* species. The derived pattern, characteristic of *H. heidelbergensis* and *H. neanderthalensis* populations, is characterized by a rhomboidal occlusal polygon and a skewed external outline, with a bulging protrusion of the hypocone in the distolingual corner (Fig. 7). The correlation coefficient (0.63) obtained, demonstrates that the cusp configuration influences the external contour shape.

The similarity between the M^1 of European middle Pleistocene populations and *H. neanderthalensis* is in accordance with other dental (Bermúdez de Castro, 1987, 1988, 1993; Martinón-Torres, 2006) and anatomical evidence (e.g., Hublin, 1982, 1984, 1996; Stringer, 1985, 1993; Arsuaga et al., 1993, 1997). Our results support the idea that M^1 shape is derived in *H. neanderthalensis*, as suggested by Bailey (2004), when compared to *Australopithecus* and early *Homo* species. However, this trait is not exclusive to Neandertals but is also characteristic of the European middle Pleistocene populations such as those recovered from Atapuerca-Sima de los Huesos, Pontnewydd, and Steinheim, although with less pronounced morphologies in the latter. While previous studies were less conclusive in assessing the relationship between *H. heidelbergensis* and *H. neanderthalensis* (Bailey, 2000), the inclusion of the large dental sample from Atapuerca-Sima de los Huesos site, has been crucial to this conclusion. As we can see in the PCA and the CVA analyses, the Arago specimens display a slightly more primitive conformation than do the rest of the *H. heidelbergensis* and *H. neanderthalensis* groups, in accordance with the "intermediate" dental morphology pointed out in previous studies (Bermúdez de Castro et al., 2003). Still, our study confirms that the M^1 morphology of the European late early Pleistocene and middle Pleistocene populations was differentiated towards the Neanderthal lineage.

Many dental traits, like other anatomical features, are highly variable within and between populations (Scott and Turner, 1997), and they frequently show quasi-continuous variation (Grüneberg, 1952). It is not easy to establish breakpoints of expression that apply to all species. In addition, it is difficult to find traits that are shared by all the members of a group and only by the members of that group. However, if a species occupies a morphospace in which only individuals of that species can be found, we can assume that specimens falling in that area probably belong to that particular group. The principal components graph (Fig. 3) illustrates considerable overlap between species in the central area. However, on the right side of the graph we find an area in which only *H. heidelbergensis* and *H. neanderthalensis* specimens and three specimens assigned to *H. antecessor* can be found. Therefore, we could interpret this morphology as derived and typical of the European middle Pleistocene populations and *H. neanderthalensis*, and its origin can be traced back in the late early Pleistocene populations of Europe. This exclusive morphospace is also confirmed by the CVA analysis. As we can see in Fig. 5, *H. heidelbergensis* and *H. neanderthalensis* occupy an exclusive spectrum (the derived morphology), clearly differentiated from the African specimens distribution (the primitive morphology). *H. sapiens* occupies an intermediate position and shows considerable overlap with the African species, as we can see in the PCA graph.

The great similarity among the upper first molars of *H. heidelbergensis* and *H. neanderthalensis* is particularly striking taking into account the new ages of the Atapuerca-SH site, which have provided an average date of 600 kyr for the site with a minimun age of 530 kyr (Bischoff et al., 2007). The M^1 shape, along with many other dental traits (Bermúdez de Castro, 1987, 1988, 1993; Martinón-Torres, 2006; Martinón-Torres et al., 2006) have demonstrated the unquestionable relationship between the hominins of Atapuerca-SH and the late

Fig. 7. Morphological comparison of three upper first molars, showing the primitive morphology of *H. sapiens* (squared occlusal polygon with regular outline) and the derivate morphology of *H. neanderthalensis* and *H. heidelbergensis* (skewed occlusal polygon with a bulging hypocone that protrudes in the outline). (a) *H. neanderthalensis* (Krapina 100); (b) *H. heidelbergensis* (AT-2071); (c) *H. sapiens* (Medieval modern human collection from San Nicolás, Murcia, Spain).

Pleistocene classic Neandertals (e.g., Arsuaga et al., 1993, 1997; Bermúdez de Castro, 1993; Martinón-Torres, 2006). The increasing evidence for the relationship between the European middle Pleistocene populations and *H. neanderthalensis*, together with the new Atapuerca-SH ages, compel us to reconsider the models of Neandertal origins. In this context, the Sima de los Huesos sample will be crucial for understanding the evolutionary scenario of Europe during the middle Pleistocene and the evolution of the Neandertals.

As we can draw from the CVA and the assignment test, M^1 morphology provides limited ability to correctly assign isolated specimens from the Pliocene and early Pleistocene to their species. These species' distributions overlap by presenting a primitive occlusal pattern with a squared and wide occlusal polygon together with a regular contour (Fig. 5). However, M^1 morphology is a very useful marker for differentiating *H. neanderthalensis* from other hominin species, especially *Homo sapiens*. This is particularly important to determining the taxonomic attribution of isolated specimens recovered from European late Pleistocene sites (Smith, 1976; Klein, 1999; Bailey, 2002, 2004; Harvati, 2003).

Allometry

Our analysis finds that there is a small but significant allometric variation in M^1 morphology that accounts for 3.02% of the observed variation. Larger molars tend to present more regular contours and more squared polygons, whereas smaller molars tend to display a centered, compressed, and rhomboidal occlusal polygon (Fig. 6).

Given that larger molars usually belong to more primitive species (Bermúdez de Castro and Nicolás, 1995), it could be hypothesized that the reduction of M^1 size in later *Homo* species was accompanied by a relative shortening of the protocone-metacone axis. However, this allometric effect is very small, so it cannot be considered responsible for the morphological variation. Despite the small centroid size in modern species (*H. sapiens*, *H. neanderthalensis*, and *H. heidelbergensis*), the

fact that *H. sapiens* tends to overlap with more primitive specimens in its general M^1 morphology prevents us from identifying an allometric factor as responsible for *H. heidelbergensis* and *H. neanderthalensis* morphology.

Evolutionary inferences

It is difficult to assess whether this characteristic Neandertal molar shape reflects any advantage or environmental adaptation. Although we are inclined to think that the particular upper first molar shape of Neandertals is the result of genetic drift, other factors may be at work. *H. neanderthalensis* facial morphology has been cited as derived in this species relative to the primitive morphology attributed to the earlier *Homo* species (Rak, 1986), and changes in the architectural facial conformation have been associated with changes in the masticatory apparatus and biomechanical questions (Hylander and Johnson, 1992; O'Connor et al., 2004). We hypothesize that the relatively distal displacement of the lingual cusps could be related to changes in dental occlusion that are correlated with the facial changes.

Geometric morphometric analyses of P_4 morphology have confirmed that *H. heidelbergensis* and *H. neanderthalensis* have fixed plesiomorphic traits in high percentages, whereas modern humans have developed a derived pattern (Martinón-Torres *et al.*, 2006). In contrast, this study reveals that *H. heidelbergensis* and *H. neanderthalensis* presents the derived pattern for the M^1 and *H. sapiens* retains the primitive condition. The differences in the evolutionary tendency of P_4 and M^1 might illustrate a process of mosaic evolution in which different skeletal parts change at different evolutionary paces. It is important to take this into account when drawing evolutionary conclusions from isolated remains.

Conclusions

Through the application of geometric morphometric methods to a large sample of African and European Pliocene and Pleistocene specimens, we have verified that *H. neanderthalensis* M^1 morphology is derived relative to *Australopithecus* and early *Homo* specimens. This derived morphology consists of a rhomboidal occlusal polygon in which lingual cusps are distally displaced and the hypocone protrudes in the external outline. In contrast, *H. sapiens* retains the primitive shape, with an approximately squared occlusal polygon and a regular contour in which no cusp protrudes in the external outline. In addition, we have demonstrated that this derived morphology is not exclusive to *H. neanderthalensis* but is already present in the European early Pleistocene populations and is characteristic of middle Pleistocene populations (*H. heidelbergensis*). The morphological differences in M^1 shape between *H. sapiens* and *H. heidelbergensis*/*H. neanderthalensis* can be useful for the taxonomic assignment of isolated late Pleistocene remains. This paper emphasizes the ability of geometric morphometric techniques to precisely assess morphological differences among species. Given the enormous potential of this methodology, future studies should explore other dental classes, searching for taxonomic and phylogenetic signals. In addition, the results of this type of analyses will be improved by their application to 3D conformations, avoiding in this way possible complications derived from the analysis of 2D images.

Acknowledgements

We are grateful to all members of the Atapuerca research team. Special thanks to the Sima de los Huesos excavation team for their arduous and exceptional contribution. We also thank D. Lordkipanidze, A. Vekua, and G. Kiladze from the Georgian National Museum; C. Bernis and J. Rascón from Universidad Autónoma de Madrid; J. Galbany from the Universidad de Barcelona; J. Svoboda and M. Oliva from the Institute of Archaeology-Paleolithic and Paleoethnology Research Center, Dolní Vestonice, Czech Republic; E. Baquedano from the Museo Arqueológico Regional de la Comunidad de Madrid, Spain; J. E. Egocheaga from the Universidad de Oviedo; and I. Tattersall, K. Mowbray, and G. Sawyer from the American Museum of Natural History, New York for providing access to the studied material and their helpful assistance when examining it. Special thanks go to James Rohlf at SUNY, Stony Brook, who has kindly revised the manuscript and made some useful comments regarding methodological aspects. We are grateful to Ana Muela and Susana Sarmiento for their technical support and for photographing part of the sample. We also thank the three anonymous reviewers for their comments on this manuscript. This research was supported by funding from the Dirección General de Investigación of the Spanish M.E.C., Project No. CGL2006-13532-C03-03/BTE, Spanish Ministry of Science and Education, Fundación Atapuerca, and Fundación Duques de Soria. Fieldwork at Atapuerca is supported by Consejería de Cultura y Turismo of the Junta de Castilla y León. This research was partly carried out under the Cooperation Treaty between Spain and the Republic of Georgia, hosted by the Fundación Duques de Soria and the Georgian National Museum.

References

Adams, D.C., Rohlf, F.J., Slice, D.E., 2004. Geometric morphometrics: ten years of progress following the 'Revolution'. Ital. J. Zool. 71, 5–16.

Albrecht, G.H., 1980. Multivariate analysis and the study of form with special reference to canonical variate analysis. Am. Zool. 20, 679–693.

Andrews, P., 1984. An alternative interpretation of the characters used to define *Homo erectus*. Cour. Forsch. Inst. Senckenb. 69, 167–175.

Arsuaga, J.L., Martínez, I., Gracia, A., Carretero, J.M., Carbonell, E., 1993. Three new human skulls from the Sima de los Huesos Middle Pleistocene site in Sierra de Atapuerca, Spain. Nature 362, 534–537.

Arsuaga, J.L., Martínez, I., Gracia, A., Lorenzo, C., 1997. The Sima de los Huesos crania (Sierra de Atapuerca, Spain). A comparative study. J. Hum. Evol. 33, 219–281.

Bailey, S.E., 2000. Dental morphological affinities among late Pleistocene and recent humans. Dent. Anthropol. 14, 1–8.

Bailey, S.E., 2002. A closer look at Neanderthal postcanine dental morphology: I. the mandibular dentition. New Anat. 269, 148–156.

Bailey, S.E., 2004. A morphometric analysis of maxillary molar crowns of Middle-Late Pleistocene hominins. J. Hum. Evol. 47, 183–198.

Bailey, S.E., Lynch, J.M., 2005. Diagnostic differences in mandibular P4 shape between Neandertals and anatomically modern humans. Am. J. Phys. Anthropol. 126, 268–277.

Bastir, M., Rosas, A., Kuroe, K., 2004. Petrosal orientation and mandibular ramus breadth: evidence of a developmental integrated petroso-mandibular unit. Am. J. Phys. Anthropol. 123, 340–350.

Bastir, M., Rosas, A., Sheets, D.H., 2005. The morphological integration of the hominoid skull: a Partial Least Squares and PC analysis with morphogenetic implications for European Mid-Pleistocene mandibles. In: Slice, D. (Ed.), Modern Morphometrics in Physical Anthropology. Kluwer Academic/Plenum Publishers, New York.

Bastir, M., Rosas, A., O'Higgins, P., 2006. Craniofacial levels and the morphological maturation of the human skull. J. Anat. 209, 637–645.

Bermúdez de Castro, J.M., 1987. Morfología comparada de los dientes humanos fósiles de Ibeas (Sierra de Atapuerca, Burgos). Estud. Geol. 43, 309–333.

Bermúdez de Castro, J.M., 1988. Dental remains from Atapuerca/Ibeas (Spain) II. Morphology. J. Hum. Evol. 17, 279–304.

Bermúdez de Castro, J.M., 1993. The Atapuerca dental remains: new evidence (1987–1991 excavations) and interpretations. J. Hum. Evol. 24, 339–371.

Bermúdez de Castro, J.M., Nicolás, E., 1995. Posterior tooth size reduction in hominids: the Atapuerca evidence. Am. J. Phys. Anthropol. 96, 335–356.

Bermúdez de Castro, J.M., Arsuaga, J.L., Carbonell, E., Rosas, A., Martínez, I., Mosquera, M., 1997. A hominid from the Lower Pleistocene of Atapuerca, Spain: possible ancestor to Neandertals and modern humans. Science 276, 1392–1395.

Bermúdez de Castro, J.M., Martinón-Torres, M., Sarmiento, S., Lozano, M., 2003. Gran Dolina-TD6 versus Sima de los Huesos dental samples from Atapuerca: evidence of discontinuity in the European Pleistocene population? J. Archaeol. Sci. 30, 1421–1428.

Biggerstaff, R.H., 1969. The basal area of posterior tooth crown components: the assessment of within tooth variation of premolars and molars. Am. J. Phys. Anthropol. 31, 163–170.

Bischoff, J.L., Williams, R.W., Rosenbauer, R.J., Aramburu, A., Arsuaga, J.L., García, N., Cuenca-Bescós, G., 2007. High-resolution U-series dates from the Sima de los Huesos hominids yields 600 kyrs: implications for the evolution of the early Neanderthal lineage. J. Archaeol. Sci. 34, 763–770.

Bookstein, F.L., 1989. Principal warps: thin-plate splines and the decomposition of deformations. IEEE T. Pattern Anal. 11, 567–585.

Bookstein, F.L., 1991. Morphometric Tools for Landmark Data. Cambridge University Press, Cambridge.

Bookstein, F.L., 1996a. Combining the tools of geometric morphometrics. In: Marcus, L.F., Corti, M., Loy, A., Naylor, G.J.P., Slice, D. (Eds.), Advances in Morphometrics. Plenum Press, New York, pp. 131–151.

Bookstein, F.L., 1996b. Applying landmark methods to biological outline data. In: Mardia, K.V., Gill, C.A., Dryden, I.L. (Eds.), Image Fusion and Shape Variability Techniques. Leeds University Press, Leeds.

Bookstein, F.L., 1997. Landmark methods for forms without landmarks: morphometrics of group differences in outline shape. Med. Image Anal. 1, 225–243.

Bookstein, F.L., Schäfer, K., Prossinger, H., Seidler, H., Fieder, M., Stringer, C., Weber, G.W., Arsuaga, J.L., Slice, D.E., Rohlf, F.J., Recheis, W., Mariam, A.J., Marcus, L.F., 1999. Comparing frontal cranial profiles in archaic and modern Homo by morphometric analysis. Anat. Rec. (New Anat.) 257, 217–224.

Bookstein, F.L., Sampson, P.D., Connor, P.D., Streissguth, A.P., 2002. Midline corpus callosum is a neuroanatomical focus of fetal alcohol damage. Anat. Rec. (New Anat.) 269, 162–174.

Bookstein, F.L., Gunz, P., Mitteroecker, P., Prossinger, H., Schaefer, K., Seidler, H., 2003. Cranial integration in Homo: singular warp analysis of the midsagittal plane in ontogeny and evolution. J. Hum. Evol. 44, 167–187.

Butler, P.M., 1963. Tooth morphology and primate evolution. In: Brothwell, D.L. (Ed.), Dental Anthropology. Symposium Publications Division, Pergamon Press, New York.

Bytnar, J.A., Trinkaus, E., Falsetti, A.B., 1994. A dental comparison of Middle Paleolithic Near Eastern hominids. Am. J. Phys. Anthropol. 19, 63.

Dahlberg, A.A., 1971. Penetrance and expressivity of dental traits. In: Dahlberg, A.A. (Ed.), Dental Morphology and Evolution. The University of Chicago Press, Chicago, pp. 257–262.

Dubois, E., 1894. *Pithecanthropus erectus*: eine menschenaehnlich Uebergangsform aus Java. Landsdrukerei, Batavia.

Dryden, I.L., Mardia, K.V., 1998. Statistical Shape Analysis. Wiley, Chichester.

Foley, R., Lahr, M., 1997. Mode 3 technologies and the evolution of modern humans. Camb. Archaeol. J. 7, 3–36.

Frieß, M., 2003. An application of the relative warps analysis to problems in human paleontology – with notes on raw data quality. Image Anal. Stereol. 22, 63–72.

Gabunia, L.K., de Lumley, M.A., Vekua, A., Lordkipanidze, D., de Lumley, H., 2002. Découverte d'un nouvel hominidé a Dmanisi (Transcaucasie, Géorgie). C.R. Palevol. 1, 243–253.

Gharaibeh, W., 2005. Correcting for the effect of orientation in geometric morphometric studies of side-view images of human heads. In: Slice, D.E. (Ed.), Modern Morphometrics in Physical Anthropology. Kluwer Academic/Plenum Publishers, New York, pp. 117–143.

González, V.M., 1990. Estudio de la dentición mandibular en la población hispano musulmana de San Nicolás (Murcia). Ph.D. Dissertation, Universidad Autónoma de Madrid.

Goose, D.H., 1963. Dental measurement: an assessment of its value in anthropological studies. In: Brothwell, D.R. (Ed.), Dental Anthropology. Pergamon, New York, pp. 125–148.

Groves, C.P., Mazák, V., 1975. An approach to the taxonomy of the Hominidae: gracile Villafranchian hominids of Africa. Casopis Min. Geol. 20, 225–247.

Grüneberg, H., 1952. Genetical studies on the skeleton of the mouse. IV. Quasi-continuous variations. J. Genet. 51, 95–114.

Gunz, P., Mitteroecker, P., Bookstein, F.L., 2005. Semilandmarks in three dimensions. In: Slice, D. (Ed.), Modern Morphometrics in Physical Anthropology. Kluwer Academic/Plenum Publishers, New York, pp. 73–98.

Harvati, K., 2003. First Neanderthal remains from Greece: the evidence from Lakonis. J. Hum. Evol. 45, 465–473.

Hillson, S., 1986. Teeth. Cambridge University Press, Cambridge.

Hillson, S., FitzGerald, C., Flinn, H., 2005. Alternative dental measurements: proposals and relationships with other measurements. Am. J. Phys. Anthropol. 126, 413–426.

Hlusko, L.J., 2004. Protostylid variation in Australopithecus. J. Hum. Evol. 46, 579–594.

Hublin, J.J., 1982. Les ante néandertaliens: présapiens our prénéandertaliens? Géobios. Mem. Spec. 6, 345–357.

Hublin, J.J., 1984. The fossil man from Salzgitter-Lebenstedt (FRG) and its place in the human evolution during the Pleistocene in Europe. Z. Morphol. Anthropol. 75, 45–56.

Hublin, J.J., 1996. The first Europeans. Archaeology 49, 36–44.

Hublin, J.J., 2001. Northwestern African Middle Pleistocene hominids and their bearing on the emergence of *Homo sapiens*. In: Barham, L., Robson-Brown, K. (Eds.), Human Roots: Africa and Asia in the Middle Pleistocene. Western Academic and Specialist Press, Bristol, pp. 99–121.

Hylander, W.L., Johnson, K.R., 1992. Strain gradients in the craniofacial region of primates. In: Davidovitch, Z. (Ed.), The Biological Mechanism of Tooth Movement and Craniofacial Adaptation. Ohio State University College of Dentistry, Columbus, Ohio, pp. 559–569.

Irish, J.D., 1993. Biological affinities of Late Pleistocene through modern African aboriginal populations: the dental evidence. Ph.D. Dissertation, Arizona State University.

Irish, J.D., 1997. Characteristic high- and low-frequency dental traits in sub-Saharan African populations. Am. J. Phys. Anthropol. 102, 455–467.

Irish, J.D., 1998. Ancestral dental traits in recent sub-Saharan Africans and the origins of modern humans. J. Hum. Evol. 34, 81–98.

Irish, J.D., Guatelli-Steinberg, D., 2003. Ancient teeth and modern human origins: an expanded comparison of African Plio-Pleistocene and recent world dental samples. J. Hum. Evol. 45, 113–144.

Klein, R.G., 1999. The Human Career. University of Chicago Press, Chicago.

Lahr, M., Foley, R., 1998. Towards a theory of modern human origins: geography, demography, and diversity in recent human evolution. Yearb. Phys. Anthropol. 41, 137–176.

Lalueza, C., Pérez-Pérez, A., 1993. The diet of the Neanderthal Child Gibraltar 2 (Devil's Tower) through the study of the vestibular striation pattern. J. Hum. Evol. 24, 29–41.

Larsen, C.S., Kelley, M.A., 1991. Introduction. In: Kelley, M.A., Larsen, C.S. (Eds.), Advances in Dental Anthropology. Wiley-Liss, New York, pp. 1–5.

Le Gros Clark, W.E., 1950. Hominid characters of the Australopithecine dentition. J. R. Anthropol. Inst. Gr. Brit. Ir. 80, 37–54.

Lozano, M., Bermúdez de Castro, J.M., Martinón-Torres, M., Sarmiento, S., 2004. Cutmarks on fossil human anterior teeth of the Sima de los Huesos Site (Atapuerca, Spain). J. Archaeol. Sci. 31, 1127–1135.

Mantel, N.A., 1967. The detection of disease clustering and a generalized regression approach. Cancer Res. 27, 209–220.

Mardia, K.V., Kent, J.T., Bibby, J.M., 1979. Multivariate Analysis. Academic Press, London.

Martinón-Torres, M., 2006. Evolución del aparato dental en homínidos: Estudio de los dientes humanos del Pleistoceno de la Sierra de Atapuerca (Burgos). Ph.D. Dissertation, Santiago de Compostela University.

Martinón-Torres, M., Bastir, M., Bermúdez de Castro, J.M., Gómez, A., Sarmiento, S., Muela, A., Arsuaga, J.L., 2006. Hominin lower second premolar morphology: evolutionary inferences through geometric morphometric analysis. J. Hum. Evol. 50, 523–533.

Mayhall, J.T., 2000. Dental morphology: techniques and strategies. In: Katzenberg, M.A., Saunders, S.R. (Eds.), Biological Anthropology of the Human Skeleton. Wiley-Liss, New York, pp. 103–134.

Mitteroecker, P., Gunz, P., Bernhard, M., Schaefer, K., Bookstein, F.L., 2004. Comparison of cranial ontogenetic trajectories among great apes and humans. J. Hum. Evol. 46, 679–698.

Mitteroecker, P., Gunz, P., Bookstein, F.L., 2005. Heterochrony and geometric morphometrics: a comparison of cranial growth in *Pan paniscus* versus *Pan troglodytes*. Evol. Dev. 7, 244–258.

Molnar, S., 1971. Human tooth wear, tooth function and cultural variability. Am. J. Phys. Anthropol. 34, 175–190.

Morris, D.H., 1986. Maxillary molar occlusal polygons in five human samples. Am. J. Phys. Anthropol. 70, 333–338.

Nolte, A.W., Sheets, H.D., 2005. Shape based assignment tests suggest transgressive phenotypes in natural sculpin hybrids (Teleostei, Scorpaeniformes, Cottidae). Front. Zool. 2, 11.

O'Connor, C.F., Franciscus, R.G., Holton, N.E., 2004. Bite force production capability and efficiency in Neandertals and modern humans. Am. J. Phys. Anthropol. 127, 129–151.

O'Higgins, P., 2000. The study of morphological variation in the hominid fossil record: biology, landmarks and geometry. J. Anat. 197, 103–120.

Pérez, S.I., Bernal, V., Gonzalez, P.N., 2006. Differences between sliding semi-landmark methods in geometric morphometrics, with an application to human craniofacial and dental variation. J. Anat. 208, 769–784.

Pérez-Pérez, A., Espurz, V., Bermúdez de Castro, J.M., de Lumley, M.A., Turbón, D., 2003. Non-occlusal dental microwear variability in a sample of Middle and Late Pleistocene human populations from Europe and the Near East. J. Hum. Evol. 44, 497–513.

Rak, Y., 1986. The Neandertal: a new look at an old face. J. Hum. Evol. 15, 151–164.

Rightmire, G.P., 1998. Human evolution in the Middle Pleistocene: the role of *Homo heidelbergensis*. Evol. Anthropol. 6, 218–227.

Rohlf, F.J., 1996. Morphometric spaces, shape components and the effects of linear transformations. In: Marcus, L.F. (Ed.), Advances in Morphometrics. Plenum Press, New York, pp. 117–128.

Rohlf, F.J., 1998a. TpsRelw. Ecology and Evolution. SUNY, Stony Brook, New York. Available online at: http://life.bio.sunysb.edu/morph/.

Rohlf, F., 1998b. TpsRegr. Ecology and Evolution. SUNY, Stony Brook, New York. Available online at: http://life.bio.sunysb.edu/morph/.

Rohlf, F., 1998c. TpsDig. Ecology and Evolution. SUNY, Stony Brook, New York. Available online at: http://life.bio.sunysb.edu/morph/.

Rohlf, F., 1998d. TpsPLS. Ecology and Evolution. SUNY, Stony Brook, New York. Available online at: http://life.bio.sunysb.edu/morph/.

Rohlf, F., 1998e. TpsUtil. Ecology and Evolution. SUNY, Stony Brook, New York. Available online at: http://life.bio.sunysb.edu/morph/.

Rohlf, F.J., 2003. Bias and error in estimates of mean shape in geometric morphometrics. J. Hum. Evol. 44, 665–683.

Rohlf, F.J., Marcus, L.F., 1993. A revolution in morphometrics. Tree 8–4, 129–132.

Rohlf, F.J., Slice, D., 1990. Extensions of the Procrustes method for the optimal superimposition of landmarks. Syst. Zool. 39, 40–59.

Scott, G.R., Turner II, C.G., 1997. The Anthropology of Modern Human Teeth: Dental Morphology and its Variation in Recent Human Populations. Cambridge University Press, Cambridge.

Sheets, H.D., 2001. Imp, Integrated Morphometric Package. Available online at: http://www.canisius.edu/~sheets/morphsoft.html.

Sheets, D.H., Kim, K., Mitchel, C.E., 2004. A combined landmark and outline-based approach to ontogenetic shape change in the Ordovician trilobite *Triarthrus becki*. In: Elewa, A. (Ed.), Morphometrics. Applications in Biology and Paleontology. Springer-Verlag, Berlin Heidelberg, pp. 67–82.

Slice, D., 2001. Landmark coordinates aligned by Procrustes analysis do not lie in Kendall's shape space. Syst. Biol. 50, 141–149.

Smith, F., 1976. The Neandertal remains from Krapina. Univ. Tenn. Dept. Anthropol. Rep. Invest. 15, 1–359.

Sneath, P.H.A., 1967. Trend-surface analysis of transformation grids. J. Zool. 151, 65–122.

Stojanowski, C.M., 2007. Comment on "Alternative dental measurements" by Hillson, et al. Am. J. Phys. Anthropol. 132, 234–237.

Stringer, C.B., 1984. The definition of *Homo erectus* and the existence of the species in African and Europe. Cour. Forsch. Inst. Senckenb. 69, 131–143.

Stringer, C.B., 1985. Middle Pleistocene hominid variability and the origin of Late Pleistocene humans. In: Delson, E. (Ed.), Ancestors: The Hard Evidence. Alan R. Liss, New York, pp. 289–296.

Stringer, C.B., 1993. Secrets of the pit of the bones. Nature 362, 501–502.

Stringer, C., 2002. Modern human origins: progress and prospects. Philos. Trans. R. Soc. London Ser B 357, 563–579.

Stringer, C., Hublin, J.J., 1999. New age estimates for the Swanscombe hominid, and their significance for human evolution. J. Hum. Evol. 37, 873–877.

Tattersall, I., Schwartz, J.H., 1999. Hominids and hybrids: the place of Neanderthals in human evolution. Proc. Natl. Acad. Sci. 96, 7117–7119.

Thomason, J., 1997. Functional Morphology in Vertebrate Paleontology. Cambridge University Press, Cambridge.

Tobias, P.V., 1991. Olduvai Gorge. The skulls endocasts and teeth of *Homo habilis*. In: Parts V–IX, vol. 4. Cambridge University Press, Cambridge.

Trinkaus, E., 1978. Bilateral asymmetry of human skeletal nonmetric traits. Am. J. Phys. Anthropol. 49, 315–318.

Turner II, C.G., 1969. Microevolutionary interpretations from the dentition. Am. J. Phys. Anthropol. 30, 421–426.

Turner II, C.G., Nichol, C.R., Scott, G.R., 1991. Scoring procedures for key morphological traits of the permanent dentition: the Arizona State University Dental anthropology system. In: Kelley, M., Larsen, C. (Eds.), Advances in Dental Anthropology. Wiley Liss, New York, pp. 13–31.

Waddington, C.H., 1957. The Strategy of the Genes. Allen and Unwin, London.

Walker, A., Leakey, R.E., 1993. The Nariokotome *Homo erectus* Skeleton. Harvard University Press, Cambridge.

Weidenreich, F., 1937. The dentition of *Sinanthropus pekinensis*; a comparative odontography of the hominids. Palaeontol. Sin. New Ser. D. 1. The Geological Survey of China.

Wolpoff, M.H., 1971. Metric Trends in Hominid Dental Evolution. Press of Case Western Reserve University, Cleveland.

Wood, B.A., 1984. The origin of *Homo erectus*. Cour. Forsch. Inst. Senckenb. 69, 99–111.

Wood, B.A., Abbott, S.A., Graham, S.H., 1983. Analysis of the dental morphology of Plio-Pleistocene hominids: II. Mandibular molars-study of cusp areas, fissure pattern and cross sectional shape of the crown. J. Anat. 137, 287–314.

Wood, B.A., Engleman, C.A., 1988. Analysis of the dental morphology of Plio-Pleistocene hominids: V. Maxillary postcanine tooth morphology. J. Anat. 161, 1–35.

Wood, B.A., Uytterschaut, H., 1987. Analysis of the dental morphology of Plio-Pleistocene hominids: III. Mandibular premolar crowns. J. Anat. 154, 121–156.

Zelditch, M.L., Swiderski, D.L., Sheets, H.D., Fink, W.L., 2004. Geometric Morphometrics for Biologists: A Primer. Elsevier Academic Press, San Diego.